Thermal and Electrical Percolation Transport Behavior in Composite Materials with Oriented Binary Fillers

Jinxin Zhong[1,2,3], Zhuoyu Wang[1,2,3], Xiaokun Gu[1,2,3*], Jun Wang[1,2,3], Yuanyuan Wang[1,2,3*], and Xin Qian[4]

[1]*School of Energy and Materials, Shanghai Polytechnic University, Shanghai 201209, China*
[2]*Shanghai Engineering Research Center of Advanced Thermal Functional Materials, Shanghai Polytechnic University, Shanghai 201209, China*
[3]*Shanghai Thermophysical Properties Big Data Professional Technical Service Platform, Shanghai Polytechnic University, Shanghai 201209, China*
[4]*School of Energy and Power Engineering, Huazhong University of Science and Technology, Wuhan 430074, China*

(Received 31 May 2025; accepted manuscript online 3 June 2025)

In integrated circuit packaging, thermal interface materials (TIMs) must exhibit high thermal conductivity and electrical resistivity to prevent short circuits, enhance reliability, and ensure safety in high-voltage applications. We proposed the thermal-percolation electrical-resistive TIM incorporating binary fillers of both insulating and metallic nanowires with an orientation in the insulating polymer matrix. High thermal conductivity can be achieved through thermal percolation, while electrical non-conductivity is preserved by carefully controlling the electrical percolation threshold through metallic nanowire orientation. The electrical conductivity of the composite can be further regulated by adjusting the orientation and aspect ratio of the metallic fillers. A thermal conductivity of $10\,\mathrm{W{\cdot}m^{-1}{\cdot}K^{-1}}$ is achieved, with electrical non-conductive behavior preserved. This approach offers a pathway to realizing "thermal-percolation electrical-resistive" in hybrid TIMs, providing a strategic framework for designing high-performance TIMs.

DOI: 10.1088/0256-307X/42/8/080602 CSTR: 32039.14.0256-307X.42.8.080602

Composite materials that incorporate a polymer matrix with various inorganic fillers have become a widely accepted approach for designing thermal interface materials (TIMs), capitalizing on the distinctive properties of each filler.[1–4] Various fillers with large thermal conductivity, including Ag nanowire,[5] carbon nanotube,[6] graphite,[7,8] silicon nitride,[9] boron nitride (BN) nanotube,[10] BN nanosheets,[11] and metal nanofibers,[12] have been intensively studied. For systems with low filler volume fractions, effective medium theory (EMT) is commonly employed to describe thermal transport behavior in composites.[13,14] However, EMT fails to account for thermal transport behavior in percolating networks, as it overlooks heat exchange between fillers, a critical factor influencing TIM performance, as highlighted by percolation theory.[15,16]

A widely accepted strategy to further enhance the thermal conductivity of TIMs is to reduce thermal boundary resistances (TBRs) between fillers within the thermal percolation network, which may be achieved through the inclusion of metallic fillers. Metallic-metallic interfaces exhibit significantly lower TBRs compared to dielectric-dielectric interfaces due to electron-dominated thermal transport.[17,18] Nevertheless, TIMs must retain electrical non-conductivity for applications such as integrated circuit packaging.

Conventional strategies for achieving thermally conductive and electrically non-conductive polymer composites primarily focus on tuning the intrinsic properties of individual fillers.[19] These include controlling the morphology of insulating ceramic fillers to construct efficient thermal pathways,[20] employing complete core-shell structures to block electrical conduction via insulating coatings,[21] and designing core-shell-like structures to reduce TBRs while preserving electrical non-conductive.[22] In contrast to these material-centric approaches, our previous work introduces a novel spatial configuration strategy that manipulates the partially metallic coatings of fillers.[23] By regulating the coating fraction and coated structure of fillers, this method intentionally decouples the thermal and electrical percolation thresholds. The resulting gap between these thresholds is then exploited to achieve high thermal conductivity without compromising electrical non-conductive, offering a new route for designing advanced TIMs. However, experimental realization of a precisely controlled, partially metallic coating on insulated nanowires presents substantial challenges.

In this letter, we propose another spatial configuration strategy to achieve thermal-percolation electrical-resistive (TP-ER) by incorporating oriented binary fillers composed of both insulating and metallic nanowires. The introduction of metallic nanowires effectively reduces the

*Corresponding authors. Email: xiaokun.gu@sspu.edu.cn; wangyuanyuan@sspu.edu.cn
© 2025 Chinese Physical Society and IOP Publishing Ltd. All rights, including for text and data mining, AI training, and similar technologies, are reserved.

TBRs within the thermal percolation network by replacing some dielectric-dielectric contacts with dielectric-metallic and metallic-metallic contacts. To enhance the thermal conductivity of TIMs while preserving electrical nonconductive, the orientation range of fillers has been carefully controlled to prevent the formation of an electrical percolating network while establishing a thermal percolating network. An intensive study on the thermal and electrical percolation behavior in composites with oriented binary fillers establishes this approach as a promising pathway to achieving high-performance TIMs.

Figure 1 illustrates the system of TIM used in our simulation. It contains two types of nanowires with different aspect ratio; one is metallic nanowire and the other is dielectric nanowire. The binary nanowires are embedded in a uniform insulating polymer matrix either randomly or oriented in a certain range with a preference to one direction. We choose SiC and Ag nanowires in the following calculation. When the filling fraction of SiC fillers (φ) is above the structural percolation threshold (φ_c), conduction networks of SiC fillers are formed, which can be considered as a heat flow network. Therefore, the percolation threshold of heat current $\varphi_c^{th} = \varphi_c$. Moreover, the thermal conductivity will be enhanced if SiC nanowire tend to aligned along the direction considered for thermal transport. At this moment, the introduction of Ag nanowires with low aspect ratio not only connects the isolated SiC clusters to form new infinite clusters,[24] but also effectively reduces the TBRs between fillers in thermal percolation network. In this case, there are three kinds of interfaces between contacted fillers: SiC-SiC, Ag-SiC, and Ag-Ag. The thermal resistance of these three interfaces can be estimated as follows. (1) For SiC-SiC direct contact, phonons are the heat carriers and the thermal resistance is $R_{\text{SiC-SiC}}/\delta_{\text{SiC-SiC}}$ where $R_{\text{SiC-SiC}}$ is the TBR of SiC-SiC interface and $\delta_{\text{SiC-SiC}}$ is the average contact area of SiC-SiC interface. (2) For Ag-SiC contact, the thermal resistance is $R_{\text{Ag-SiC}}/\delta_{\text{Ag-SiC}}$ where $R_{\text{Ag-SiC}}$ is the TBR of Ag-SiC interface. Both electrons and phonons contribute to the TBR of Ag-SiC interface. (3) For Ag-Ag interface, the overall thermal resistance is $R_{\text{Ag-Ag}}/\delta_{\text{Ag-Ag}}$. The electrons are the major heat carriers for TBR of Ag-Ag interface. This thermal resistance is negligible compared to the previous two contacts because $R_{\text{Ag-Ag}} \ll R_{\text{Ag-SiC}} < R_{\text{SiC-SiC}}$. If Ag nanowires in the polymer matrix are oriented within a certain range of angles (as shown in Fig. 1), the electrical percolation

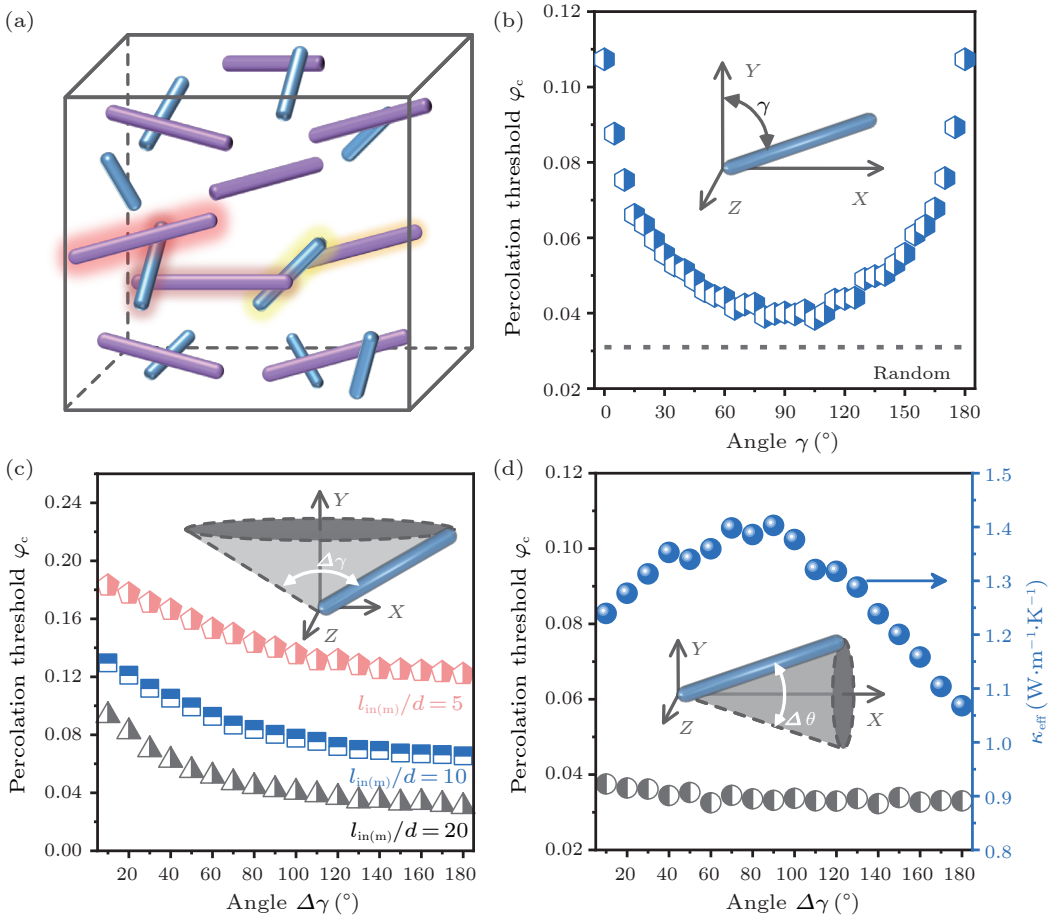

Fig. 1. (a) Schematic diagram of the concept of TP-ER with oriented binary fillers. Here we choose SiC and Ag nanowires as an example. Ag is in blue and SiC is in purple. (b) Percolation threshold φ_c versus the angle γ when $l_{in(m)}/d = 20$. The percolation threshold φ_c of systems with random orientation is plotted as dotted line. (c) Percolation threshold φ_c as a variation of $\Delta\gamma$ for different aspect ratio $l_{in(m)}/d$. (d) Percolation threshold φ_c as a variation of $\Delta\theta$ with the $l_{in}/d = 20$. κ_{eff} is evaluated along x diection with a single filler of SiC nanowires of $\varphi_{in} = 0.2$.

threshold $\varphi^{\mathrm{e}}_{\mathrm{c,oriented}}$ in the heat transport direction will strongly depend on the range of angles. The electrical percolation network would not form in the heat transport direction when $\varphi_{\mathrm{m}} < \varphi^{\mathrm{e}}_{\mathrm{c,oriented}}$. A higher electrical percolation threshold allows for the addition of more Ag fillers, which further reduces the TBRs between fillers and creates additional heat flow networks. In summary, the TP-ER concept can be realized by fulfilling $\varphi_{\mathrm{m}} < \varphi^{\mathrm{e}}_{\mathrm{c,oriented}}$ and $\varphi > \varphi^{\mathrm{th}}_{\mathrm{c}}$.

The numerical method applied for calculating thermal conductivity and electrical conductivity of composites has been detailed in the Supplementary Materials (SM) and Ref. [25]. To illustrate its validity, we also summarize in the SM a comparison with experimental data from a previous study,[5] where this model was shown to reproduce the measured properties of Ag nanowire/PVDF [poly (vinylidene fluoride)] composites. The length of the cubic simulation box is L and there are two types of nanowires with an orientation of γ or θ in it. One is the insulating SiC nanowire with length l_{in} and diameter d; the other is the metallic Ag nanowire with length l_{m} and the same diameter d. For the sake of efficiency, the length of nanowires are set as $l_{\mathrm{in(m)}}/L \leq 0.4$. When generating the position and orientation of the nanowires, the nanowires that exceed left plane ($x = 0$) and right plane $x > L$ are cut off, and the periodic boundary conditions are applied in the Y- and Z-directions.[26] In our calculations, the nanowires are treated as soft-core, as the difference between hard-core and soft-core models becomes negligible for large aspect ratios.[27] For simplicity, Ohmic contacts are assumed as the ideal case in the following calculations.[28] The electrical conductivity of the system can be obtained by applying a voltage bias on the left and right planes; then the electrical current can be obtained by adopting a resistor network algorithm and Kirchhoff's current law.[29] The system is electrically non-percolating when $\varphi_{\mathrm{m}} < \varphi^{\mathrm{e}}_{\mathrm{c,oriented}}$; the system is electrically non-conductive. Once the percolation threshold is exceeded, the electrical conductivity σ exhibits a universal power-law dependence on the excess filler concentration.[27,30]

After considering the electrical transport, we investigate the effective thermal conductivity of the composite materials. It depends on several parts: the thermal conductivity of the matrix, the thermal percolating network, and the fillers which do not belong to the network (isolated fillers and finite clusters).[31–33] Here, we focus on the contribution of the thermal percolating network and the matrix to the effective thermal conductivity because the contributions of isolated fillers and finite clusters are trivial. Thus, the effective thermal conductivity is characterized by $\kappa_{\mathrm{eff}} \approx \kappa_{\mathrm{net}} + \kappa_{\mathrm{p}}$, where κ_{net} and κ_{p} are the thermal conductivities of the thermal percolating network and matrix, respectively. Assuming the matrix is thermally insulated, the thermal conductivity of the thermal percolation network can be obtained by applying a temperature bias on the left and right planes of the system and calculating the resulting heat flow using a thermal resistor network algorithm and Fourier's law. The net heat flux of the i-th nanowire J_i is defined as

$$J_i = \sum\nolimits_j^N \left(\frac{1}{\frac{2l_i}{\kappa_i \pi d^2} + \frac{2l_j}{\kappa_j \pi d^2} + \frac{R_{\mathrm{I}}}{\delta}} \right) (T_i - T_j), \quad (1)$$

where N is the number of nanowires connected to the i-th nanowire, κ is the intrinsic thermal conductivity of nanowires, T is the temperature of nanowire, δ is the average contact area, set as $0.04d^2$ to simplify modeling, reflecting the small real contact between nanowires due to roughness and misalignment. R_{I} is the TBR between fillers. A self-consistent solution algorithm is then employed to iteratively update the i-th nanowire temperature T_i so that $J_i \to 0$ for all nanowires, ensuring local heat flux balance. The value of $R_{\mathrm{Ag\text{-}Ag}}$, $R_{\mathrm{Ag\text{-}SiC}}$ and $R_{\mathrm{SiC\text{-}SiC}}$ are taken as 2×10^{-10}, 2×10^{-9}, $1 \times 10^{-8}\,\mathrm{m^2{\cdot}KW^{-1}}$, respectively.[34–37] The PVDF was selected as the matrix material due to its high temperature tolerance and good thermal stability, and the thermal conductivity of PVDF κ_{p} is $0.19\,\mathrm{W{\cdot}m^{-1}{\cdot}K^{-1}}$.[38,39] The thermal conductivity of SiC is $490\,\mathrm{W{\cdot}m^{-1}{\cdot}K^{-1}}$,[40] and it is dielectric.[41] The aspect ratio of SiC nanowires is $l_{\mathrm{in}}/d = 20$ with $l_{\mathrm{in}} = 4\,\mu\mathrm{m}$. The electrical conductivity of Ag is $6.3 \times 10^7\,\mathrm{S/m}$.[42] The thermal conductivity of Ag is $429\,\mathrm{W{\cdot}m^{-1}{\cdot}K^{-1}}$.[5]

Figure 1(b) presents the percolation threshold φ_{c} as a function of the angle γ for an aspect ratio of $l_{\mathrm{in(m)}}/d = 20$ along the X direction. The percolation threshold φ_{c} for systems with randomly oriented nanowires is also included. We observed that φ_{c} for systems with nanowires fixed at a specific angle γ is higher than that for randomly oriented nanowires. The orientation of the nanowires significantly impacts the curvature of the conduction path ξ and the contact rate between the nanowires p. ξ quantifies the average misalignment of nanowires relative to the heat flow direction, with greater curvature indicating increased path tortuosity and associated thermal resistance. As $\varphi \to \varphi_{\mathrm{c}}$, only one conduction pathway exists within the system. Given that the angle between the i-th nanowire and the direction of conduction is α_i, ξ can be evaluated from $\frac{1}{C_{\mathrm{f}}} \sum_i^{C_{\mathrm{f}}} (1 - |\cos\alpha_i|) \approx 1 - \overline{|\cos\alpha_i|}$. Here, C_{f} denotes the number of nanowires encapsulated within this system, which can be evaluated as $\frac{1}{p} \frac{L}{l_{\mathrm{in(m)}} \overline{|\cos\alpha_i|}}$. The contact rate p is approximately positively correlated with the diversity of the orientations. Consequently, $\varphi_{\mathrm{c}} \sim C_{\mathrm{f}} \frac{4}{\pi d^2 l_{\mathrm{in(m)}}} \sim \frac{C}{p(1-\xi)}$, where the constant C is determined by $\frac{L}{l_{\mathrm{in(m)}}} \frac{4}{\pi d^2 l_{\mathrm{in(m)}}}$. A higher ξ results in a larger φ_{c} because it necessitates more nanowires to form the infinite cluster that connects the two ends in the conduction direction we considered. Additionally, a low p resulting from strong restrictions on orientation will also lead to a higher φ_{c}. Therefore, the phenomenon depicted in Fig. 1(b) arises from the combined effects of these two factors. In particular, the φ_{c} of systems with $\gamma = 90^\circ$ is higher than that of systems with random orientation, indicating that the lowering effect of low curvature is outweighed by the elevating effect of low p on φ_{c}.

If the requirement for orientation restrictions is relaxed from a specific angle with respect to a direction (γ) to a

range of angles around a certain direction (θ), the competitive effects of p and ξ can effectively offset each other. This is illustrated by the black dots in Fig. 1(d), which shows minimal change in the φ_c compared to the random case. As the preference axis of fillers changes from X to Y, the relationship between p and ξ shifts from competition to cooperation. The joint action of these two factors drives a higher φ_c compared to that of randomly oriented systems, as illustrated by the black and blue dots for $\Delta\gamma \in (10, 80)$ in Fig. 1(c). As $\Delta\gamma$ continues to increase, the combined effect of the two factors can diminish to zero. This joint action also profoundly impacts the transport behavior of the composite materials. The effective thermal conductivity κ_{eff} is determined by $\kappa_{\text{net}} \approx L/(C_f L^2 \tilde{R}_f) \sim \frac{p(1-\xi)}{\tilde{C}}$, where $\tilde{R}_f$ is the equivalent thermal resistance of the nanowires (KW^{-1}), and $\tilde{C}$ is given by $\frac{L^2}{l_{\text{in(m)}}}(\frac{4l_{\text{in(m)}}}{\kappa_f \pi d^2} + \frac{R_I}{\delta})$. A higher ξ means that the heat flow must pass through more intrinsic thermal resistance of the nanowires, resulting in a reduction of κ_{eff}. Conversely, a greater p indicates that the composite materials can form more conduction channels, enhancing κ_{eff}. Consequently, κ_{eff}, which benefits from a higher p but is inhibited by a higher ξ, exhibits an optimal value as $\Delta\theta_{\text{in}}$ increases, as shown by the blue dots in Fig. 1(d).

Figure 2(a) shows the calculated κ_{eff} as a function of φ_m and $\Delta\gamma_m$ with $\varphi_{\text{in}} = 0.2$, $l_m/d = 10$, and randomly oriented SiC nanowires. The threshold for electrical percolation is also plotted. We found that composite materials with high thermal conductivity (approximately $4.5\,\text{W}\cdot\text{m}^{-1}\cdot\text{K}^{-1}$) and electrical non-conductive can be achieved when $0° \le \Delta\gamma_m \le 40°$ and $\varphi_m > 0.1$. It is evident that κ_{eff} increases with increasing $\Delta\gamma_m$. With a fixed $\Delta\gamma_m = 20°$, the effect of Ag nanowire aspect ratio on κ_{eff} is negligible compared to that of φ_m as shown in Fig. 2(b).The aspect ratio of Ag nanowires only matters for determining the ceiling of φ_m. Additionally, κ_{eff} can be further improved by controlling the orientation of the SiC nanowires, $\Delta\theta_{\text{in}}$, when $l_m/d = 10$, $\varphi_{\text{in}} = 0.15$, and $\varphi_m = 0.15$, as shown in Fig. 2(c). A more random orientation of Ag nanowires is beneficial for achieving a larger value of κ_{eff}. As illustrated in Fig. 2(d), composite materials with high thermal conductivity (about $6\,\text{W}\cdot\text{m}^{-1}\cdot\text{K}^{-1}$) and electrical non-conductive can be achieved when $0° \le \Delta\theta_{\text{in}} \le 130°$ and $\varphi_{\text{in}} > 0.25$.

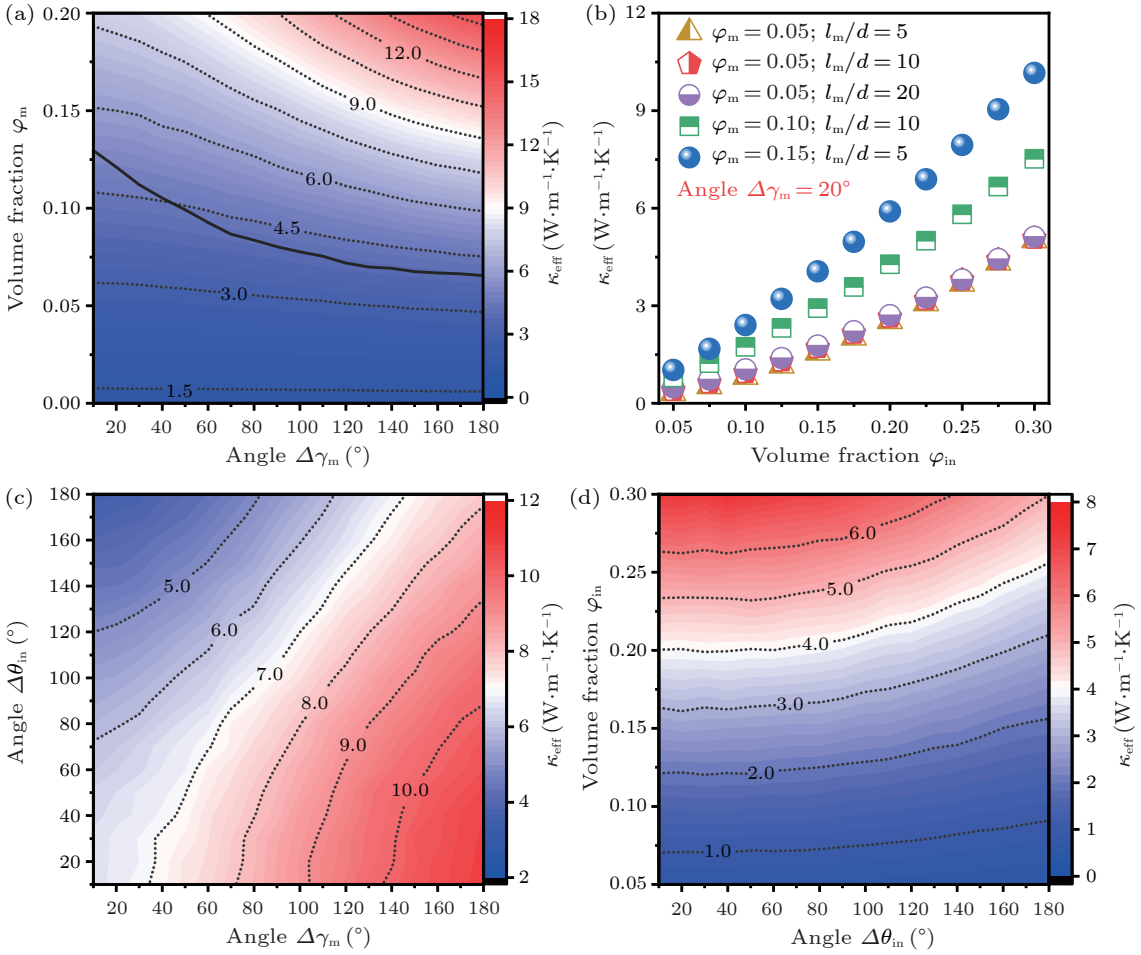

Fig. 2. (a) The calculated κ_{eff} as a function of φ_m and $\Delta\gamma_m$ with $\varphi_{\text{in}} = 0.2$, $l_m/d = 10$, and orientation of SiC nanowires is random. The black line is the modified electrical percolation threshold. (b) κ_{eff} as a vriation of φ_{in}, φ_m, and l_m/d with $\Delta\gamma_m = 20°$ and orientation of SiC nanowires is random. (c) κ_{eff} plotted as a function of $\Delta\gamma_m$ for different $\Delta\theta_{\text{in}}$ when $l_m/d = 10$, $\varphi_{\text{in}} = 0.15$, and $\varphi_m = 0.15$. (d) The calculated κ_{eff} as a function of φ_{in} and $\Delta\theta_{\text{in}}$ with $\varphi_m = 0.05$, $l_m/d = 10$, and orientation of Ag nanowires is random.

In conclusion, we have proposed a type of composite material in which binary fillers of both insulating and metallic nanowires are embedded in an insulating polymer matrix. The thermal conductivity of these composite materials with oriented nanowires exhibits an optimal value as $\Delta\theta$ increases, due to the combined effects of contact rate and curvature. Moreover, TIMs with ultra-high thermal conductivity can be achieved by controlling the orientation of both insulating and metallic nanowires. Simultaneously, electrical conductivity can be regulated through $\Delta\gamma_{\mathrm{m}}$ and the aspect ratio l_{m}/d. Our calculations demonstrate that the strategy of utilizing oriented binary fillers comprising both insulating and metallic nanowires is effective and successful in achieving efficient TIMs with ultra-high thermal conductivity and electrical non-conductive. The thermal conductivity calculated in this work is along the X direction, which can correspond to in-plane or through-plane transport in practice, allowing flexible application to various TIM configurations.

Acknowledgments. This work was supported by the National Key R&D Program (Grant No. 2022YFA1203-100). J. Zhong acknowledge sponsorship by Shanghai Sailing Program (Grant No. 24YF2713800). Y. Wang acknowledges financial support from the Local College Capacity Building Project of Shanghai Municipal Science and Technology Commission (Grant No. 20010500700), the Natural Science Foundation of Shanghai (Grant No. 23ZR1424300), and Shanghai Shuguang Program (Grant No. 22SG56).

References

[1] Bonnet P, Sireude D, Garnier B, and Chauvet O 2007 *Appl. Phys. Lett.* **91** 201910
[2] Sun K, Zhang Z, Qian L, Dang F, Zhang X, and Fan R 2016 *Appl. Phys. Lett.* **108** 061903
[3] Zheng R, Gao J, Wang J, Feng S P, Ohtani H, Wang J, and Chen G 2012 *Nano Lett.* **12** 188
[4] Song S H, Park K H, Kim B H, Choi Y W, Jun G H, Lee D J, Kong B S, Paik K W, and Jeon S 2013 *Adv. Mater.* **25** 732
[5] Shi B, Dong L, Li M, Liu B, Kim K, Xu X, Zhou J, and Liu J 2018 *Appl. Phys. Lett.* **113** 041902
[6] Haggenmueller R, Guthy C, Lukes J R, Fischer J E, and Winey K I 2007 *Macromolecules* **40** 2417
[7] Min C, Yu D, Cao J, Wang G, and Feng L 2013 *Carbon* **55** 116
[8] Hung M T, Choi O, Ju Y S, and Hahn H 2006 *Appl. Phys. Lett.* **89** 023117
[9] Zhou W, Wang C, Ai T, Wu K, Zhao F, and Gu H 2009 *Composites Part A: Applied Science and Manufacturing* **40** 830
[10] Jo I, Pettes M T, Kim J, Watanabe K, Taniguchi T, Yao Z, and Shi L 2013 *Nano Lett.* **13** 550
[11] Wu Y, Zhang X, Negi A, He J, Hu G, Tian S, and Liu J 2020 *Polymers* **12** 426
[12] Zeng J, Cao Z, Yang D, Sun L, and Zhang L 2010 *J. Therm. Anal. Calorim.* **101** 385
[13] Zhao Y, Zeng X, Ren L, Xia X, Zeng X, and Zhou J 2021 *Mater. Chem. Front.* **5** 5617
[14] Nan C W, Liu G, Lin Y, and Li M 2004 *Appl. Phys. Lett.* **85** 3549
[15] Kargar F, Barani Z, Salgado R, Debnath B, Lewis J S, Aytan E, Lake R K, and Balandin A A 2018 *ACS Appl. Mater. Interfaces* **10** 37555
[16] Zhong J, Xi Q, Jin H, Wang Z, Ma D, Liu J, and Zhou J 2022 *Appl. Phys. Lett.* **121** 162201
[17] Liu B, Dong L, Xi Q, Xu X, Zhou J, and Li B 2018 *Front. Energy* **12** 72
[18] Wang Q, Liang X, Liu B, Song Y, Gao G, and Xu X 2020 *Nanoscale* **12** 1138
[19] Chen Q, Yang K, Feng Y, Liang L, Chi M, Zhang Z, and Chen X 2024 *Composites Part A: Applied Science and Manufacturing* **178** 107998
[20] Yan Q, Dai W, Gao J *et al.* 2021 *Acs Nano* **15** 6489
[21] Zhou Y, Liu F, and Chen C Y 2019 *Adv. Compos. Hybrid Ma.* **2** 46
[22] Tong Y z, Zhao W j, Wu W, Zhang D l, He G j, Yang Z T, and Cao X w 2022 *Adv. Compos. Hybrid Ma.* **5** 263
[23] Zhong J, Xi Q, He J, Liu J, and Zhou J 2021 *Appl. Phys. Lett.* **119** 211602
[24] Rahatekar S S, Shaffer M S, and Elliott J A 2010 *Compos. Sci. Technol.* **70** 356
[25] Liu B, Lu T, Wang B, Liu J, Nakayama T, Zhou J, and Li B 2017 *Appl. Phys. Lett.* **110** 113102
[26] SongW, Krishnaswamy V, and Pucha R V 2016 *Compos. Struct.* **137** 9
[27] Foygel M, Morris R, Anez D, French S, and Sobolev V 2005 *Phys. Rev. B* **71** 104201
[28] Choi D Y, Kang H W, Sung H J, and Kim S S 2013 *Nanoscale* **5** 977
[29] Kirkpatrick S 1973 *Rev. Mod. Phys.* **45** 574
[30] Nakayama T, Yakubo K, and Orbach R L 1994 *Rev. Mod. Phys.* **66** 381
[31] Huxtable S T, Cahill D G, Shenogin S, Xue L, Ozisik R, Barone P, Usrey M, Strano M S, Siddons G, Shim M *et al.* 2003 *Nat. Mater.* **2** 731
[32] Malekpour H, Chang K H, Chen J C, Lu C Y, Nika D, Novoselov K, and Balandin A 2014 *Nano Lett.* **14** 5155
[33] Yu A, Ramesh P, Sun X, Bekyarova E, Itkis M E, and Haddon R C 2008 *Adv. Mater.* **20** 4740
[34] Gundrum B C, Cahill D G, and Averback R S 2005 *Phys. Rev. B* **72** 245426
[35] Swartz E T and Pohl R O 1989 *Rev. Mod. Phys.* **61** 605
[36] Monachon C, Weber L, and Dames C 2016 *Annu. Rev. Mater. Res.* **46** 433
[37] Zhong J, Xi Q, Wang Z, Nakayama T, Li X, Liu J, and Zhou J 2021 *J. Appl. Phys.* **129** 195102
[38] Han Z and Fina A 2011 *Prog. Polym. Sci.* **36** 914
[39] Xi Q, Zhong J, He J, Xu X, Nakayama T, Wang Y, Liu J, Zhou J, and Li B 2020 *Chin. Phys. Lett.* **37** 104401
[40] Nilsson O, Mehling H, Horn R, Fricke J, and Hofmann R 1997 *High Temp.-High Pressures* **29** 73
[41] Gradinaru G, Sudarshan T, Gradinaru S, Mitchell W, and Hobgood H 1997 *Appl. Phys. Lett.* **70** 735
[42] Wang S, Tian Y, Hang C, and Wang C 2018 *Sci. Rep.* **8** 5260